An Occlusion Detection System for Intravenous Infusion

Lianqiao Zhou, Qinlan Li, Liyang Wang, Mengjie Wang, Longfei Li, Bo Ding, Shengwen Bao, Shugang Wang, Xiaobing Xiao, Jingqiang Cui, Guosheng Wang, Chong Liu, and Yewang Su

***Abstract*—Infusion pumps play a pivotal role in the medical field, ensuring the continuous and precisely controlled delivery of medications or nutrients. However, occlusions in the intravenous lines (IV lines) pose significant hurdles for infusion pump employment, which impact treatment effectiveness and even endanger patients' lives. The conventional methods for detecting occlusions in IV lines do not simultaneously meet the requirements for noninvasiveness, high accuracy, and high consistency. Here, we report a design for a pressure waveform sensor (PWS) with a waveform-based recognition method to detect IV lines occlusions. To overcome the technical challenges, several attempts including the double-clamped beam structure and the waveform template matching algorithm (WTMA) are exploited in this work. The mechanical and electrical characteristics of the PWS are verified by theoretical analysis, numerical analysis, and experiments. Finally, the PWS with the WTMA is validated in commercial electrical infusion pumps, demonstrating no false positive alarms (FPAs) observed among a total injection volume of 80 000 mL across ten infusion pumps with 50 infusion bags. The result underscores the tremendous potential of the system for IV lines occlusion detection.**

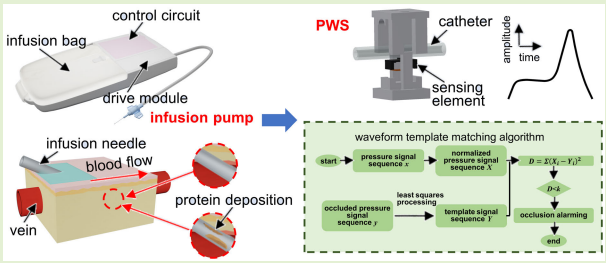

***Index Terms*— High consistency, infusion pumps, intravenous lines (IV lines) occlusions, pressure sensors, waveform-based recognition method.**

Manuscript received 25 August 2023; accepted 15 September 2023. Date of publication 25 September 2023; date of current version 31 October 2023. This work was supported in part by the National Natural Science Foundation of China under Grant 12172359, in part by the Key Research Program of Frontier Sciences of the Chinese Academy of Sciences under Grant ZDBS-LY-JSC014, and in part by the Chinese Academy of Sciences (CAS) Interdisciplinary Innovation Team under Grant JCTD-2020-03. The associate editor coordinating the review of this article and approving it for publication was Prof. Kai Wu. *(Corresponding author: Yewang Su.)*

Lianqiao Zhou and Qinlan Li are with the State Key Laboratory of Nonlinear Mechanics, Institute of Mechanics, Chinese Academy of Sciences, Beijing 100190, China, and also with the School of Engineering Science, University of Chinese Academy of Sciences, Beijing 100049, China.

Liyang Wang, Mengjie Wang, Longfei Li, Bo Ding, Shengwen Bao, Shugang Wang, Xiaobing Xiao, Jingqiang Cui, and Guosheng Wang are with the Henan Key Laboratory of Medical Polymer Materials Technology and Application, Tuoren Medical Device Research and Development Institute Company Ltd., Xinxiang, Henan 453000, China.

Chong Liu is with the State Key Laboratory of High-Temperature Gas Dynamics, Institute of Mechanics, Chinese Academy of Sciences, Beijing 100190, China.

Yewang Su is with the State Key Laboratory of Nonlinear Mechanics, Institute of Mechanics, Chinese Academy of Sciences, Beijing 100190, China, also with the School of Engineering Science, University of Chinese Academy of Sciences, Beijing 100049, China, and also with the Beijing Key Laboratory of Engineered Construction and Mechanobiology, Institute of Mechanics, Chinese Academy of Sciences, Beijing 100190, China (e-mail: yewangsu@imech.ac.cn).

This article has supplementary downloadable material available at https://doi.org/10.1109/JSEN.2023.3317074, provided by the authors.

Digital Object Identifier 10.1109/JSEN.2023.3317074

I. Introduction

INFUSION pumps, which generate flow by deforming a specific soft catheter in a manner, have been widely applied in the medical field because of the precise dose controlled, long-term infusion, and lower contamination degree for the isolation between the fluid and mechanical parts of the pump [1]. An estimated 90% of hospital patients [2] receives nutrients or medications via infusion pumps in nearly all types of surgery and treatment [3], [4], [5], [6], [7], [8], [9], [10], [11], [12], [13], [14], [15]: hormones like insulin in diabetes treatment [5], antibiotics in colon resection and peripheral vascular reconstruction [4], chemotherapy drugs in cancer [6] and blood disorders [9], and pain relievers in the spine and other complex orthopedic. Due to a variety of reasons including a protein deposition at the end of a needle tip, a filter clogging, a folded or compressed infusion catheter section, or a pinch clamp malfunction, the occlusion occurs in relatively high frequency among all infusion pump alarms [16]. In most medical applications, unnoticed occlusion will reduce clinical outcomes for insufficient drug delivery and risk patients' life for the bolus injected under the dangerous pressure buildup in the catheter [17], [18], [19]. Therefore, it is extremely significant to detect occlusion during the long-term infusion process.

The optimal occlusion detection system faces several requirements/challenges.

1) *Noninvasiveness:* Any contact between the fluid and sensing element will increase the risk of contamination.
2) *Accuracy and Consistency:* The occlusion detection system needs to accurately identify the unobstructed and occluded conditions within the intravenous lines (IV lines), while minimizing the influence of manufacturing, assembly errors, or mechanical motion.
3) *Low Alarm Delay:* The occlusion detection system needs to raise an alarm as quickly as possible after occlusion occurs.
4) *Low Power Consumption:* Portable infusion pumps typically operate for several days, necessitating the sensing and data processing components with minimal power consumption.
5) *Low Cost and Ease of Installation:* The occlusion detection sensor needs to be reusable and feature easily installable components to reduce costs and alleviate the burden on the medical staff.

According to the requirements mentioned above, several strategies for occlusion detection in clinics have certain limitations. For example, thermal flow sensors [20] have high power consumption, flow sensors with deflecting structures [21] are invasive in essence, and ultrasonic transit time flow sensors [22], [23] have complex processing circuitry and high cost. Therefore, hydraulic pressure sensors [24], [25], [26], [27], [28], [29], [30], [31] with a priority of noninvasiveness, lower power consumption, and lower cost have a promising future in IV lines occlusion detection. The majority of these hydraulic pressure sensors detect pressure changes directly by utilizing an ultrathin diaphragm integrated with the catheter [24], [30]. However, the ultrathin diaphragm asks for a careful installment of the catheter, which increases the complication of the installation. In addition to utilizing the ultrathin diaphragm, it is feasible to measure the hydraulic pressure changes within IV lines by monitoring the expansion of a catheter section wall. Based on the variations in hydraulic pressure, an algorithm known as the pressure threshold algorithm (PTA) is utilized to differentiate the occlusion condition of IV lines. Nonetheless, the measurement of the hydraulic pressure changes also relies on the elastic modulus and geometry parameters of the catheter, as well as the preload applied during installation. Thus, the discrepancies in these parameters, caused by the process of manufacturing and assembly, result in the elevation of false alarm rates. In conclusion, finding a practical and suitable solution for occlusion detection within IV lines remains challenging.

In this work, we report a pressure waveform sensor (PWS) with a waveform-based recognition method, which satisfies the above four requirements simultaneously and can be integrated into commercial infusion pumps for detecting occlusions online. The PWS consists of a housing, deformation substrate, and strain gauge to detect pressure change. To overcome the technical challenges and satisfy the requirements in applications, noninvasive design, normalization operation, and waveform template matching algorithm (WTMA) are exploited in this work. The mechanical and electrical characteristics of the PWS are verified by theoretical analysis, numerical analysis, and experiments. Furthermore, the PWS with the WTMA is incorporated into commercial electrical infusion pumps to verify its effectiveness on IV lines occlusion detection. The results indicate that the PWS exhibits no false positive alarms (FPAs) even when the total infusion volume reaches 80 000 mL. This outcome suggests the potential of the system to effectively detect occlusions within IV lines.

II. Sensing Principle

A. Display and Mechanism of the Infusion Pump and the PWS

Fig. 1(a) shows the usage scenario of the electrical infusion pumps in the intravenous transfusion. The infusion pumps usually consist of three parts: an infusion bag, a control circuit, and a drive module. The inset exhibits one kind of infusion procedure [32]. In the beginning, the left slider and middle slider compress the tube. When the middle slider moves down to create a low-pressure area, the fluid is sucked in from the inlet driven by the pressure difference. Then, the right slider moves up and compresses the catheter to prevent fluid reflux. As the middle slider moves up and the left slider moves down, the fluid extrudes out of the outlet driven by the pressure difference. Repeating the above steps, the fluid will flow out continuously. However, in certain scenarios, such as protein deposition [see Fig. 1(b)], the injection channel occludes, which will affect the treatment effect and endanger patients' life. Thus, it is necessary to detect the occlusion accurately and alarms as soon as possible. During a single infusion cycle, the hydraulic pressure within the catheter changes corresponding to the movement of the sliders in the infusion pump. If the IV line nonoccludes, the liquid will flow out quickly, which induces small pressure changes [see Fig. 1(c)]. On the other hand, if the IV line occludes, the liquid will accumulate within the catheter resulting in higher pressure levels and fluctuations [see Fig. 1(d)]. To obtain the hydraulic pressure changes within the catheter, a PWS is supposed to install along the tube. Fig. 1(e) shows three major parts of the PWS: a housing for clamping the catheter, a deformation substrate with a double-clamped beam structure to convert the pressure to the deformation, and a strain gauge to measure the strain of the substrate. To preserve the performance of the PWS in the complex environments, a protective encapsulation layer is applied to safeguard the strain gauge. When the catheter is occluded, the hydraulic pressure drives the expansion of the catheter wall, leading to the deformation of the substrate. Then, the strain gauge bonded to the lower surface of the substrate deforms, resulting in resistance changes. Fig. 1(f) shows the pressure sensor and the deformation substrate.

B. Design, Mechanical, and Electrical Characterization of the PWS

The sensing element design dominates the performance of the PWS. Here, a double-clamped beam structure with a bulge is adopted to convert the hydraulic pressure within the catheter to the deformation of the sensing element [details shown in

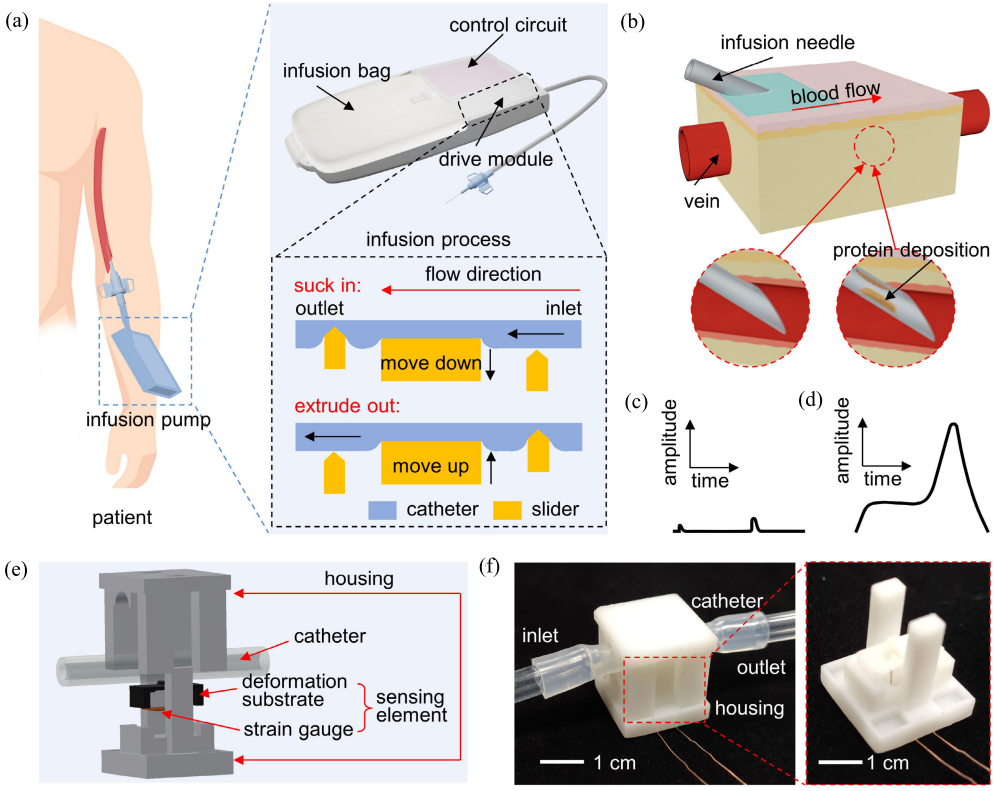

Fig. 1. Schematic illustrations for the application, operation principle of infusion pumps, the dynamic fluctuations of hydraulic pressure within the catheter, and images of a PWS. (a) Application of an electrical infusion pump for nutrients or medication delivery (inset: component of the infusion pump and the illustration of the sliders' movement within a single infusion cycle). (b) Intravenous therapy model (inset: enlarged view of the needle tip with and without the protein deposition). (c) and (d) Dynamic fluctuations of hydraulic pressure observed within IV lines under the conditions of nonocclusion and occlusion. (e) Exploded view of a designed PWS. (f) Optical image of a fabricated PWS.

Fig. 2(a)]. The inner radius of the catheter is denoted as r_i and the outer radius is denoted as r_o. The thickness of the beam t and the width of the bulge w impact the bending stiffness and strain distribution of the sensing element. The finite element analysis (FEA) result exhibits a higher strain on the both side of the bulge, while a lower strain at the bottom of the bulge (the hydraulic pressure is set to 0.15 MPa, about 1100 mmHg). Fig. 2(b) shows the relationship between the average strain $\bar{\varepsilon}_x$ in the bonding section of the strain gauge and the radio of width to thickness w/t. As w/t increases, the average strain $\bar{\varepsilon}_x$ increases for the decrease in bending stiffness. When w/t exceeds 1.6, the average strain $\bar{\varepsilon}_x$ starts to decrease due to the lower contact area with the catheter. Therefore, the substrate with $w/t = 1.6$ is employed. To obtain an analytical solution relating the electrical output of the PWS to the hydraulic pressure within the catheter, it is necessary to investigate the mechanical characteristics of the substrate. Due to the complexity of the substrate structure, the FEA is applied. Fig. 2(c) illustrates the relationship between the applied pressure and the average strain $\bar{\varepsilon}_x$, as well as the relationship between the applied pressure and the substrate displacement u_y. Based on the results, the stiffness coefficient of the substrate is determined as $k = 3.097 \times 10^4$ (MPa/mm), and the pressure-strain coefficient is determined as $s = 1.9 \times 10^{-3}$ (MPa^{-1}). Considering the geometric character and the small deformation hypothesis, the deformation process is simplified as plane strain model [32]. In the quasi-static process, the analytical relationship between the hydraulic pressure within the expansion section of the catheter and the pressure applied on the substrate is derived as (details shown in the text in the Supporting Information)

$$\frac{p_o}{p_i} = \frac{\left[(1-\nu^*)r_i^2 - (1+\nu^*)r_i r_o\right]}{\frac{E^*(r_o+r_i)}{2k} - \left[(1+\nu^*)r_i r_o - (1-\nu^*)r_o^2\right]} \tag{1}$$

where p_o is the contact pressure caused by the housing and sensing element, p_i is the hydraulic pressure within the catheter, r_i is the inner radius, r_o is the outer radius, k is the stiffness coefficient of the substrate, $E^* = E/(1-\nu^2)$, and $\nu^* = \nu/(1-\nu)$, where E is Young's modulus of the catheter and ν is Poisson's ratio. Based on the principle of the strain gauge resistance variation, the relative resistance change is expressed as $\Delta R/R_0 = K \cdot s \cdot p_o$, where K is the gauge factor of the strain gauge and s is the pressure-strain coefficient. Fig. 2(d) depicts the analytical and experimental results on the relationship between the relative resistance change $\Delta R/R_0$ and the applied hydraulic pressure within the catheter. Further details can be found in Fig. S1a and Section III. In the pressure range of 0–0.15 MPa, the relationship demonstrates a satisfied linearity with the goodness-of-fit $R^2 = 0.99$. Here, R_0 and ΔR represent the original resistance of the PWS and its increment due to the applied hydraulic pressure, respectively. Because of the rapid completion of a single infusion cycle within a few

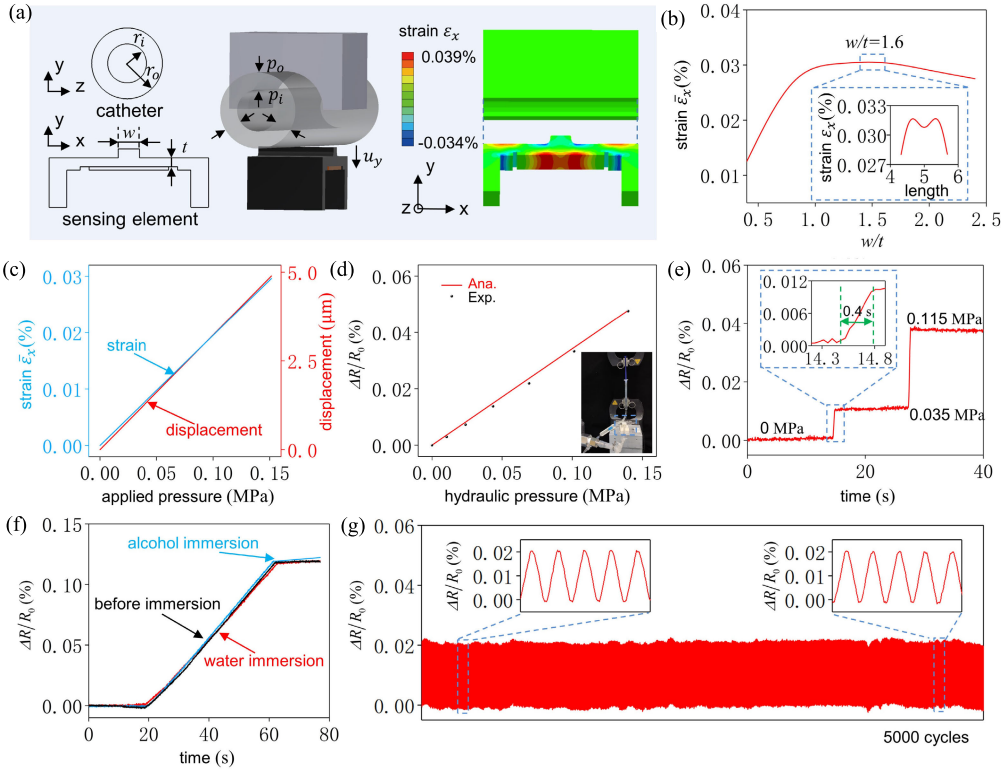

Fig. 2. Design, mechanical, and electrical characterization of the PWS. (a) Mechanical model of the PWS. The geometry parameters of the catheter and the sensing element (left). The 3-D model of the PWS (middle). FEA results of the strain ε_x distribution (right). (b) Curve of the average strain $\bar{\varepsilon}_x$ under different w/t values. Inset: strain distribution ε_x when $w/t = 1.6$. (c) Average strain $\bar{\varepsilon}_x$ and displacement response of the substrate. (d) Relative resistance changes of the PWS versus the hydraulic pressure in the catheter. (e) Relative resistance changes for step loads from 0 MPa to 0.035, 0.115, and 0.220 MPa. Inset: response time about 0.4 s. (f) Effect of the water and alcohol immersion on the relative resistance changes of the PWS versus the hydraulic pressure. (g) Relative resistance changes under repeated loading and unloading of hydraulic pressure about 0.06 MPa for 5000 cycles.

seconds, it is crucial for the PWS to exhibit a robust dynamic response to detect pressure variations accurately. Fig. 2(e) illustrates the results of a step load test conducted on the PWS. As the step load increases from 0 MPa to 0.035 and 0.115 MPa, the output increases sharply at first and then remains. For instance, the output stabilizes within 0.4 s when the step load is 0.035 MPa. To assess the output stability in severe environments, the PWS is immersed in water and alcohol for 24 h, substances commonly used in the medical field (details shown in Fig. S2). The gauge factor of the PWS exhibits minimal variation before and after immersion, as depicted in Fig. 2(f). The result indicates that the PWS is well-suited for operation in the medical environment. Furthermore, stability is also very important for practical applications of the PWS. As demonstrated in Fig. 2(g), the performances, including applied hydraulic pressure range (0–0.06 MPa), repeatability, and linearity, remain over a span of 5000 loading and unloading cycles.

C. Mechanism of IV Lines Occlusion Detection

To quantitatively investigate the relationship between hydraulic pressure fluctuations induced by the infusion process and the output of the PWS, a simple yet effective theoretical model is established. The catheter and PWS are simplified as the model shown in Fig. 3(a). Here, the catheter is consisted of two parts: the one in higher Young's modulus exposed out of the PWS and the other one in lower Young's modulus connected with the PWS directedly and denoted as the expansion section. The controllable clamp is used to exert compression on the end of the catheter to simulate the occlusion section. q_i represents the volume flow rate in the inlet, p_i represents the hydraulic pressure in the expansion section of the catheter, P_0 represents the atmospheric pressure, V represents the infusion volume per cycle, and r_1, r_2, r_3, and r_4 represent the inner radius of the catheter in the inlet section, expansion section, outlet section, and occlusion section, respectively. The liquid, like medicine or nutrients, driven by the infusion pump, flows through the inlet into the soft catheter and then flows out through the outlet. As the clamp compresses the catheter, the liquid accumulates, resulting in the wall expansion. During the infusion process, the substrate undergoes deformation as a result of hydraulic pressure transmitted through the catheter wall. Due to the complexity of the multiphysical couple in directly analyzing the substrate deformation, an indirect analysis model [see Fig. 3(b)] is introduced here according to the lumped parametric model [33], [34], [35], [36], [37], [38], [39], [40], [41]. For a catheter in which the laminar flow of an incompressible fluid develops, the fluid resistance caused by the viscous forces can be given in theoretical as $R = 8\mu l/\pi r^4$, where μ is the fluid viscosity coefficient, l is the length, and r is the inner radius. An approximate expression for the capacitance in a fluid system caused by the elasticity

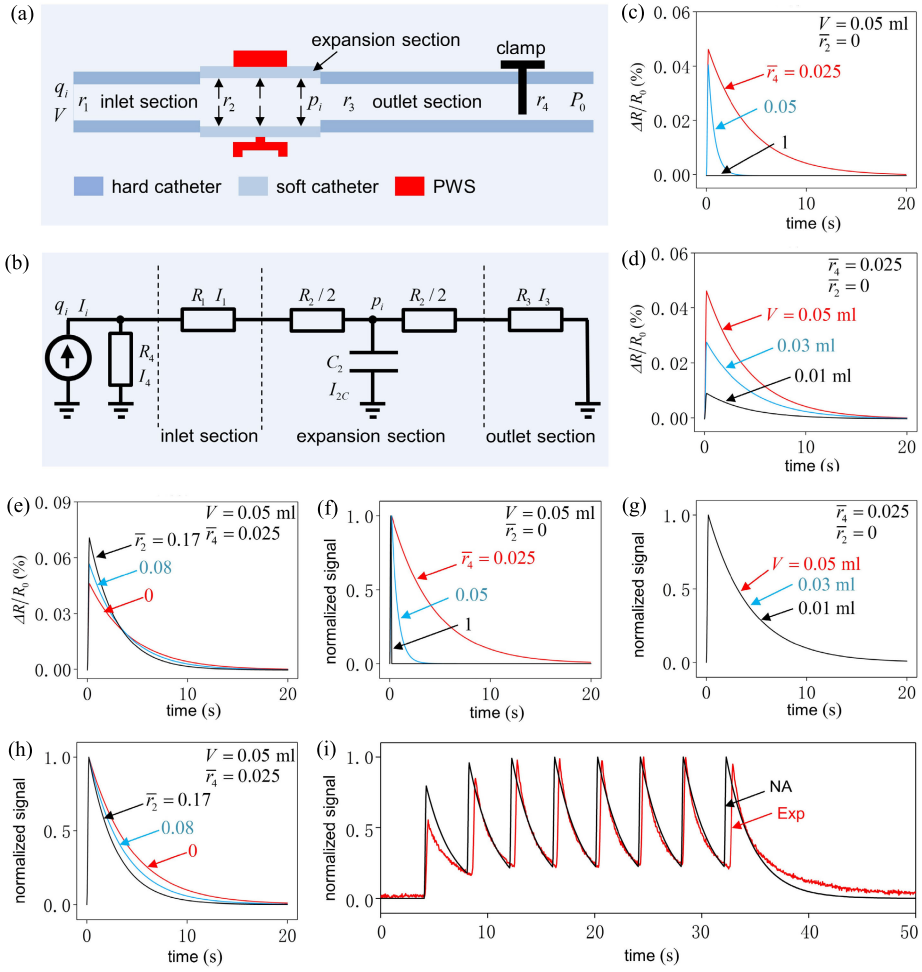

Fig. 3. Mechanism of IV lines occlusion detection. (a) Illustration of the equivalent simplified model for the catheter, PWS, and occlusion. (b) Lumped parametric model of the infusion process. Curves of the relative resistance change within a single infusion cycle under three different conditions: (c) $V = 0.05$ mL, $\bar{r}_2 = 0$, and $\bar{r}_4 = 0.025$, 0.05, and 1; (d) $\bar{r}_4 = 0.025$, $\bar{r}_2 = 0$, and $V = 0.05$, 0.03, and 0 mL; and (e) $\bar{r}_4 = 0.025$, $V = 0.05$ mL, and $\bar{r}_2 = 0.17$, 0.08, and 0. Curves of the normalized signal within a single infusion cycle under three different conditions: (f) $V = 0.05$ mL, $\bar{r}_2 = 0$, and $\bar{r}_4 = 0.025$, 0.05, and 1; (g) $\bar{r}_4 = 0.025$, $\bar{r}_2 = 0$, and $V = 0.05$, 0.03, and 0 mL; and (h) $\bar{r}_4 = 0.025$, $V = 0.05$ mL, and $\bar{r}_2 = 0.17$, 0.08, and 0. (i) Comparison of the normalized signal obtained from the numerical model and experimental results in continuous infusion cycles.

of the thick wall catheter can be given as

$$C = 2\pi l r_i^2 r_o^2 \{[(1-\nu^*)r_i^2/r_o^2 - (1+\nu^*)] + 2\nu^* p_o/p_i\}/[E^*(r_o^2 - r_i^2)]$$

the details are shown in the text in the Supporting Information. Furthermore, the inertia effect in the short catheter is so smaller than the resistance and capacitance that can be neglected in later analysis. As the Young modulus of the catheter is higher in the inlet and outlet than in the expansion section, the capacitance in the inlet and outlet can be disregarded for simplify. The phenomenon of reflux occurs when the hydraulic pressure within the catheter exceeds the driving pressure exerted by the infusion pump. Therefore, the infusion pump is modeled as a nonideal current source, which is consisted of an ideal current source and an inside resistance in parallel connection. According to Kirchhoff's laws, the analytical relationship between the volume flow rate q_i and the hydraulic pressure within the expansion section can be obtained using the lumped parametric model as follows:

$$I_i = q_i, \quad I_i = I_4 + I_1, \quad I_1 = I_{2C} + I_3 \tag{2}$$

$$\left(R_1 + \frac{R_2}{2}\right)\frac{\mathrm{d}}{\mathrm{d}t}(I_1) + \frac{I_{2C}}{C_2} - R_4\frac{\mathrm{d}}{\mathrm{d}t}(I_4) = 0$$

$$\left(\frac{R_2}{2} + R_3\right)\frac{\mathrm{d}}{\mathrm{d}t}(I_3) - \frac{I_{2C}}{C_2} = 0 \tag{3}$$

where I_i represents the volume flow generated by the infusion pump; I_1, I_3, I_{2C}, and I_4 represent the volume flow going through the inlet, outlet, expansion section, and inside resistance, respectively; R_1, R_2, and R_3 are the resistances of the inlet, expansion, and outlet section, respectively; R_4 is the inside resistance of the infusion pump; C_2 is the fluid capacitance of the catheter expansion section. Based on the initial condition $I_1 = I_3 = I_4 = 0$, the voltage in the capacitance can be calculated as $U_C = \int I_{2C}/C_2 \mathrm{d}t$, which is equivalent to the hydraulic pressure p_i in the expansion section (details shown in the text in the Supporting Information). By combining (1) with (2) and (3), the relationship between

the relative resistance change $\Delta R/R_0$ of the PWS and the volume flow rate q_i can be established. The numerical analysis results are illustrated as follows.

The electrical response varies according to different parameters of the infusion system, including the infusion volume per cycle, and the inner radius of the expansion section and occlusion section, which reflects the assembly errors and occlusion degree, respectively. With the constant $V = 0.05$ mL and $\bar{r}_2 = 1 - r_2/r_1 = 0$, Fig. 3(c) shows the numerical result of the relative resistance change $\Delta R/R_0$ with the decrease of $\bar{r}_4 = r_4/r_1$ within a single infusion cycle. Here, $\bar{r}_2$ represents the assembly errors and $\bar{r}_4$ represents the openness of the catheter. When the outlet is totally unobstructed ($\bar{r}_4 = 1$), the hydraulic pressure within the catheter is insufficient to cause the wall deformation, resulting in a relatively stable output signal. However, as the openness decreases to 0.025, the output signal increases initially, reaching its peak, and then gradually decreases to zero. For different $\bar{r}_4$ values, the peak value and decay time of the output signal vary. With the constant $\bar{r}_4 = 0.025$ and $\bar{r}_2 = 0$, Fig. 3(d) shows the variation of the relative resistance change $\Delta R/R_0$ with different infusion volumes per cycle V. As V increases, the residual fluid volume within the catheter also increases, resulting in greater catheter wall deformation and higher output signal. For example, the peak value under the condition of $V = 0.05$ mL is around three times as large as that under the condition of $V = 0.01$ mL. With the constant $V = 0.05$ mL and $\bar{r}_4 = 0.025$, the peak value of the relative resistance change $\Delta R/R_0$ increases with the increment of $\bar{r}_2$ due to the less fluid volume storage in the expansion section [details shown in Fig. 3(e)]. Therefore, relying solely on the peak value of the output signal for discerning the occlusion condition (like PTA) is unreliable. To address this technical challenge, a normalized operation is implemented during the data processing phase [as depicted in Fig. 3(f)–(h)]. Following the normalization process, the output signals in different occlusion conditions still exhibit a sharp increase to the peak, but their subsequent decrease occurs at varying rates, resulting in distinct pressure waveforms. For different infusion volumes per cycle V and assembly errors $\bar{r}_2$, the output signals demonstrate great consistency. Consequently, it is more reliable and accurate to differentiate the occlusion condition based on the normalized pressure waveform. What is more, the infusion speed is determined by both the infusion volume per cycle and the time gap between infusion cycles. Because the time gap between infusion cycles will not impact the pressure changes within a single infusion cycle, the infusion speed does not affect the performance of the occlusion detection system. Finally, the numerical analysis results are validated by the experimental results (after normalization) under the conditions of nearly occlusion degree and infusion volume per cycle [see Fig. 3(i)]. Both sets of results demonstrate similar increasing/decreasing rates and exhibit comparable signal waveforms.

III. Experiment Method

A. Fabrication Process of the PWS

As shown in Fig. S5, the fabrication processes of the PWS were conducted as follows. Step 1: the displacement-restricted housing and substrate were fabricated using 3-D printing technology (Mohou, China). Step 2: a strain gauge (Xing DongFang, China) was bonded to the lower surface of the substrate with an adhesive (ergo 5800, Switzerland). Step 3: silicone rubber glue (Kafuter silicon glue, K-705, China) was used to encapsulate the strain gauge. Step 4: the substrate was inserted into the housing with the adhesive (ergo 5800, Switzerland). When the PWS was installed in the infusion pump, it was supposed to replace the housing with the infusion pump case.

B. Characterization of the PWS

Static and dynamic loading tests of the PWS were carried out by the programmable tensile testing machine (MTS C42.503, Holland), and the detailed description was shown in Fig. S1b. The loading and unloading cycle tests were carried out by the programmable tensile testing machine (ZQ-990A, ZHIQU, China). The hydraulic pressure in the catheter was measured by a water pressure gauge (HC-Y810, China). The resistance and voltage signals of the sensors were measured by a data acquisition system (Keysight DAQ970A, America). The gauge factor of the strain gauge is adopted as $K = 1.8$.

C. FEAs of the Substrate Deformation

The FEA was performed employing the commercial software ABAQUS (SIMULIA, France) to analyze the performance of two kinds of models of the substrate. The displacement-restricted block and the substrate bonded a gauge strain with the boundary conditions of zero displacements imposed in all directions, and an elastic catheter with a pressure of 0.18 MPa applied in the inner wall was calculated in the FEA model. The polymer of the deformation substrate was treated as a linear elastic material, with Young's modulus of 2.7 GPa and Poisson's ratio of 0.4. PI was treated as a linear elastic material, with Young's modulus of 2.5 GPa and Poisson's ratio of 0.35. The elastic rubber of the catheter was treated as a linear elastic material, with Young's modulus of 2.6 MPa and Poisson's ratio of 0.5. All of the materials adopted the hexahedron element C3D8R.

D. Numerical Analyses of the Lumped Parametric Model in the Infusion Process

MATLAB/Simulink (MathWorks, America) analysis was performed to calculate the hydraulic pressure changes in the infusion process. The lumped parametric model exhibited in Fig. S6, where the fluid resistance caused by the viscous forces was equivalent to an electrical resistance, the elasticity of the thick wall catheter was equivalent to an electrical capacitance, the occlusion was equivalent to an electrical resistance, and the infusion pump was equivalent to an ideal current source parallel connected with an inside resistance. To simplify the input condition, the infusion flow was modeled as a sinusoidal fluctuation $V(t) = \pi V_0/2T \cdot \sin(\pi t/T)$ under the total infusion volume consistency condition. Other parameters in the model are outlined as follows: the fluid mass density $\rho = 1 \times 10^3$ kg/m^3; the fluid viscosity coefficient $\mu = 1 \times 10^{-3}$ Pa·s, infusion volume per cycle $V = 0.05$ mL, Young's moduli of the catheter are 24.21 and 1.56 MPa for the hard section and

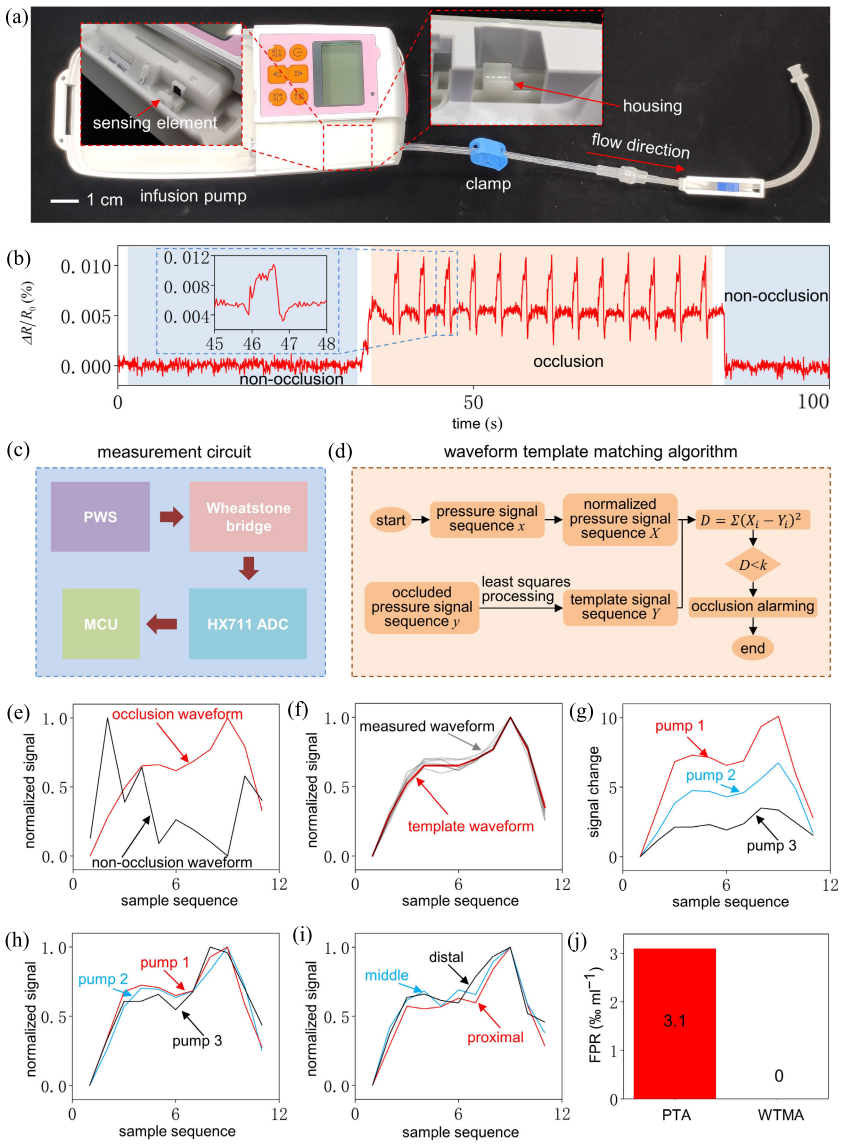

Fig. 4. Occlusion detection algorithm design and validation. (a) Image of the infusion pump incorporated with a PWS, medical catheter, and clamp. The placement of the sensing element (left inset). The placement of the housing corresponding to the sensing element (right inset). (b) Relative resistance changes of the PWS in infusion process under complete occlusion. Inset: enlarged view of the relative resistance changes within a single infusion cycle. (c) Component of the PWS measurement circuit. (d) Operating procedures of the WTMA. (e) Comparison of the normalized output signal under nonocclusion condition and occlusion condition when the sample point is 11. (f) Curves of measured waveforms and the template waveform under occlusion condition. (g) Comparison of the output signal changes of PWSs utilized in different infusion pumps under complete occlusion. (h) Comparison of the normalized output signal of PWSs utilized in different infusion pumps under complete occlusion. (i) Comparison of the normalized output signal of the PWS when the occlusion occurs in the proximal, middle, and distal sections of IV lines, respectively. (j) FPA under tradition PTA and WTMA.

soft section, respectively, Poisson's ratio of the catheter is 0.5, the inner radius $r_i = 1$ mm, and the outer radius $r_o = 1.9$ mm.

IV. Results and Discussion

To exhibit great potential of the occlusion detection system in IV lines, the PWS is integrated with a commercial infusion pump, as shown in Fig. 4(a). Here, a clamp is assigned to simulate the occlusion condition. By connecting the leads of the PWS to an ohmmeter, the relative resistance change $\Delta R/R_0$ varied during the infusion process is recorded in Fig. 4(b). When the outlet is unobstructed, no significant hydraulic pressure and fluctuations are detected. Once the clamp in the outlet closes, the hydraulic pressure increases to a high level with periodic fluctuations. In the consecutive infusion process, the waveform of the output remains, which is the basic prerequisite to distinguish the occlusion condition. If the occlusion is not severe, the hydraulic pressure can still reach a balanced state after several infusion processes (details shown in Fig. S3). To detect the occlusion condition online, a pressure measurement circuit is introduced, which consists of three constant resistances composed of a Wheatstone bridge with the PWS, an HX711 module for converting the analog signal to the digital signal, and a microcontroller unit (MCU) for data manipulation [details shown in Figs. 4(c) and S4]. In addition, a discriminating algorithm WTMA with the

evaluate criteria named diversity distance, based on waveform matching operation, is introduced. The basic operating procedures of the WTMA within a single infusion cycle is shown in Fig. 4(d).

1) To obtain the template waveform, the pressure changes under the occlusion condition are recorded by the PWS, denoted as the occluded pressure signal sequence y. A set of characteristic pressure signal sequences are obtained by repeating the step using infusion pumps from different production batches.
2) Then, the normalized template signal sequence Y can be calculated using the least squares method based on the characteristic pressure signal sequences.
3) At the time to detect IV lines occlusion condition, the pressure signal sequence x is recorded within a single infusion cycle. The normalized pressure signal sequence is denoted as X.
4) To discriminate the pressure signal sequence obtained in occlusion condition, the diversity distance is defined as $D = \sum (Y_i - X_i)^2$, where the subscript i is the serial number of the sample sequence.

When the diversity distance is below a threshold ($D < k$), it is claimed that the current pressure waveform is similar to the template waveform, which also means the catheter is under occlusion condition. Here, the threshold is selected elaborately by amounts of experimental data to achieve the better distinguish effect. Furthermore, only a characteristic waveform fragment of the output signal is used to distinguish the occlusion condition to reduce the computing load of the MCU. The pressure signal waveforms under occlusion and nonocclusion conditions with the sample points of 11 are presented in Fig. 4(e). Under the occlusion condition, the normalized signal increases to a platform at first, then climbs to the highest point, and decreases finally, which corresponds to the movement of the slider in the infusion pump. While under the nonocclusion condition, the hydraulic pressure in the catheter is so small to deform the substrate in the PWS. The normalized signal consists of irregular electrical noise or mechanical vibration noise. These huge difference in waveforms under the two conditions become the fundament of the discrimination. Fig. 4(f) illustrates the curves of the template waveform and the current pressure waveforms under occlusion conditions, with the template waveform obtained using the least squares method. As analyzed in Section III-C, the output signal of the PWS is susceptible to manufacturing and assembly errors. Fig. 4(g) demonstrates the diverse signal changes of PWSs utilized in different infusion pumps under complete occlusion. The magnitude of signal changes exhibits significant variation, highlighting the high false alarm rates associated with the conventional PTA. For instance, if the alarm pressure threshold is determined based on the signal change observed in pump 2, it is likely to result in a failure to trigger an alarm in pump 3. In other words, it is challenging to establish a consistent alarm pressure threshold due to potential manufacturing or assembly errors. However, despite these variations, the normalized signal change waveforms display a remarkable degree of consistency, as depicted in Fig. 4(h). Generally, the further location of the occlusion along the catheter results in lower pressure changes. However, after normalization, the waveforms exhibit a high degree of consistency regardless of whether the occlusion occurs in the proximal, middle, or distal section of IV lines, as shown in Fig. 4(i). This conformity in waveform patterns allows for the identification of a template waveform that represents the typical characteristics. To assess the effectiveness of the WTMA, four commercial infusion pumps were tested, with two employing the PTA and the other two employing the WTMA. Fig. 4(j) shows the false positive rate (FPR) under different processing algorithms. After the infusion volume reaching to 10 000 mL, the pumps with the PTA exhibit 31 FPAs with the FPR of 3.1‰ mL^{-1}, while the pumps with the WTMA show no FPAs, which indicates the great advantage of the WTMA. What is more, we shake and inverse the infusion pump to simulate the daily movements that might occur, and no FPAs are observed. Finally, a total of ten commercial infusion pumps with the WTMA are tested to evaluate the consistency across different production batches. Through the process of changing 50 infusion bags and infusing a total volume of 80 000 mL, no instances of FPAs are observed. Furthermore, the pumps with the WTMA demonstrate a rapid alarm trigger speed during subsequent infusion cycles following the total occlusion within the catheter, which is in accordance with the periodic fluctuations observed in Fig. 4(b).

V. Conclusion

In summary, a PWS with the WTMA for detecting the occlusion condition in real time is proposed. After the elaborated design, the PWS exhibits proper tolerance to water or alcohol immersion conditions and fatigue life. Then, a simple yet effective theoretical model is established to quantitatively investigate the relationship between hydraulic pressure fluctuations induced by the infusion process and the output of the PWS. To overcome technique challenges, key designs developed in this work include: 1) the nonintrusive construction to rule out the possibility of additional contamination; 2) the WTMA to eliminate pressure value discrepancies caused by different single injection volumes or manufacture errors and discriminate the pressure waveform under nonocclusion or occlusion condition; and 3) sample points reduction to lower the power consumption. The mechanical and electrical characteristics of the PWS are also verified by numerical analysis and experiments. Finally, the PWSs with the WTMA are incorporated into commercial electrical infusion pumps, which show no FPA among the total injection volume of 80 000 mL in ten infusion pumps with 50 infusion bags. The collective results demonstrate that the proposed PWS has promising applications in medical infusion pumps to detect occlusion conditions. In addition, based on the design principle of the PWS, it is potential for the redesign and adaptation of this sensor to address occlusion detection requirements in other applications characterized by pulsatile infusion patterns.

Appendix

Supporting Information is available from the IEEE Sensors Journal or from the author.

REFERENCES

[1] S. S. Dychter, D. A. Gold, D. Carson, and M. Haller, "Intravenous therapy: A review of complications and economic considerations of peripheral access," *J. Infusion Nursing*, vol. 35, no. 2, pp. 84–91, Mar. 2012, doi: 10.1097/NAN.0b013e31824237ce.

[2] K. K. Giuliano, "Intravenous smart pumps," *Crit. Care Nursing Clinics North Amer.*, vol. 30, no. 2, pp. 215–224, Jun. 2018, doi: 10.1016/j.cnc.2018.02.004.

[3] T. H. Kim et al., "A temporary indwelling intravascular aphaeretic system for in vivo enrichment of circulating tumor cells," *Nature Commun.*, vol. 10, no. 1, pp. 1478–1485, Apr. 2019, doi: 10.1038/s41467-019-09439-9.

[4] D. E. Fry, "Antibiotics in surgery: An overview," *Amer. J. Surg.*, vol. 155, no. 5, pp. 11–15, May 1988, doi: 10.1016/S0002-9610(88)80206-X.

[5] E. Renard, "Automated insulin delivery systems: From early research to routine care of type 1 diabetes," *Acta Diabetologica*, vol. 60, no. 2, pp. 151–161, Aug. 2022, doi: 10.1007/s00592-022-01929-5.

[6] Z. Q. Qin et al., "Continuous intravenous infusion of recombinant human endostatin using infusion pump plus chemotherapy in non-small cell lung cancer," *World J. Clin. Cases*, vol. 10, no. 4, pp. 1164–1171, Feb. 2022, doi: 10.12998/wjcc.v10.i4.1164.

[7] C. Motamed, "Clinical update on patient-controlled analgesia for acute postoperative pain," *Pharmacy*, vol. 10, no. 1, p. 22, Jan. 2022, doi: 10.3390/pharmacy10010022.

[8] D. Williams, D. Petruccelli, J. Paul, L. Piccirillo, M. Winemaker, and J. de Beer, "Continuous infusion of bupivacaine following total knee arthroplasty: A randomized control trial pilot study," *J. Arthroplasty*, vol. 28, no. 3, pp. 479–484, Mar. 2013, doi: 10.1016/j.arth.2012.07.016.

[9] G. Egerer et al., "Continuous infusion of ceftazidime for patients with breast cancer and multiple myeloma receiving high-dose chemotherapy and peripheral blood stem cell transplantation," *Bone Marrow Transplantation*, vol. 30, no. 7, pp. 427–431, Oct. 2002, doi: 10.1038/sj.bmt.1703660.

[10] P. Gibbs, A. Purushotham, C. Auld, and R. J. Cuschieri, "Continuous wound perfusion with bupivacaine for postoperative wound pain," *Brit. J. Surg.*, vol. 75, no. 9, pp. 923–924, Dec. 2005.

[11] E. E. Ashcraft et al., "Further improvements in laparoscopic donor nephrectomy: Decreased pain and accelerated recovery," *Clin. Transplantation*, vol. 15, pp. 59–61, Nov. 2001, doi: 10.1034/j.1399-0012.2001.00011.x.

[12] F. H. Savoie, L. D. Field, R. N. Jenkins, W. J. Mallon, and R. A. Phelps II, "The pain control infusion pump for postoperative pain control in shoulder surgery," *Arthroscopy*, vol. 16, no. 4, pp. 339–342, May 2000, doi: 10.1016/S0749-8063(00)90076-8.

[13] C.-C. Wu, C.-H. Bai, M.-T. Huang, C.-H. Wu, and K.-W. Tam, "Local anesthetic infusion pump for pain management following open inguinal hernia repair: A meta-analysis," *Int. J. Surg.*, vol. 12, no. 3, pp. 245–250, Mar. 2014, doi: 10.1016/j.ijsu.2014.01.006.

[14] N. H. Stringer, K. L. Rodino, M. Edwards, and N. V. A. Kumari, "On-Q system for managing trocar site pain after operative laparoscopy," *J. Amer. Assoc. Gynecologic Laparoscopists*, vol. 7, pp. 552–555, Nov. 2000, doi: 10.1016/S1074-3804(05)60374-X.

[15] J. F. Chester, K. Ravindranath, B. D. White, D. Shanahan, R. S. Taylor, and K. Lloyd-Williams, "Wound perfusion with bupivacaine: Objective evidence for efficacy in postoperative pain relief," *Ann. Roy. College Surgeon England*, vol. 71, p. 394, Nov. 1989.

[16] D. C. Klonoff, G. Freckmann, and L. Heinemann, "Insulin pump occlusions: For patients who have been around the (infusion) block," *J. Diabetes Sci. Technol.*, vol. 11, no. 3, pp. 451–454, May 2017, doi: 10.1177/1932296817700545.

[17] P. Zhang, S.-Y. Wang, C.-Y. Yu, and M.-Y. Zhang, "Design of occlusion pressure testing system for infusion pump," *J. Biomed. Sci. Eng.*, vol. 2, no. 6, pp. 431–434, 2009, doi: 10.4236/jbise.2009.26062.

[18] H. Kawakami et al., "Amount of accidental flush by syringe pump due to inappropriate release of occluded intravenous line," *Technol. Health Care*, vol. 21, no. 6, pp. 581–586, Nov. 2013, doi: 10.3233/THC-130754.

[19] D. Deckert, C. Buerkle, A. Neurauter, P. Hamm, K. H. Lindner, and V. Wenzel, "The effects of multiple infusion line extensions on occlusion alarm function of an infusion pump," *Anesthesia Analgesia*, vol. 108, no. 2, pp. 518–520, Feb. 2009, doi: 10.1213/ane.0b013e31819237ae.

[20] D. Lee et al., "Sensitive and reliable thermal micro-flow sensor for a drug infusion system," *Sens. Actuators A, Phys.*, vol. 309, Jul. 2020, Art. no. 112033, doi: 10.1016/j.sna.2020.112033.

[21] R. Hagihghi, A. Razmjou, Y. Orooji, M. E. Warkiani, and M. Asadnia, "A miniaturized piezoresistive flow sensor for real-time monitoring of intravenous infusion," *J. Biomed. Mater. Res. B, Appl. Biomaterials*, vol. 108, no. 2, pp. 568–576, Feb. 2020, doi: 10.1002/jbm.b.34412.

[22] T. Pennell, J. L. Yi, B. A. Kaufman, and S. Krishnamurthy, "Noninvasive measurement of cerebrospinal fluid flow using an ultrasonic transit time flow sensor: A preliminary study," *J. Neurosurg., Pediatrics*, vol. 17, no. 3, pp. 270–277, Mar. 2016, doi: 10.3171/2015.7.PEDS1577.

[23] M. Wang and J. Chen, "A high-precision gravity intravenous infusion rate meter using CMUT arrays," in *Proc. IEEE Int. Ultrason. Symp.*, Sep. 2009, pp. 1355–1358, doi: 10.1109/ULTSYM.2009.5441987.

[24] D. J. Apigo, P. L. Bartholomew, T. Russell, A. Kanwal, R. C. Farrow, and G. A. Thomas, "Evidence of an application of a variable MEMS capacitive sensor for detecting shunt occlusions," *Sci. Rep.*, vol. 7, no. 1, pp. 1–9, Apr. 2017, doi: 10.1038/srep46039.

[25] M. Cescon et al., "Early detection of infusion set failure during insulin pump therapy in type 1 diabetes," *J. Diabetes Sci. Technol.*, vol. 10, no. 6, pp. 1268–1276, Nov. 2016, doi: 10.1177/1932296816663962.

[26] A. Facchinetti, S. Favero, G. Sparacino, and C. Cobelli, "An online failure detection method of the glucose sensor-insulin pump system: Improved overnight safety of type-1 diabetic subjects," *IEEE Trans. Biomed. Eng.*, vol. 60, no. 2, pp. 406–416, Feb. 2013, doi: 10.1109/TBME.2012.2227256.

[27] P. Herrero et al., "Robust fault detection system for insulin pump therapy using continuous glucose monitoring," *J. Diabetes Sci. Technol.*, vol. 6, no. 5, pp. 1131–1141, Sep. 2012, doi: 10.1177/193229681200600518.

[28] S. M. Gouveia, "In-line pressure monitoring in IV infusions: Benefits for patients and nurses," *Brit. J. Nursing*, vol. 25, no. 19, pp. 28–33, Oct. 2016, doi: 10.12968/bjon.2016.25.19.S28.

[29] F. Doesburg, R. Oelen, M. H. Renes, P. M. Lourenço, D. J. Touw, and M. W. Nijsten, "Multi-infusion with integrated multiple pressure sensing allows earlier detection of line occlusions," *BMC Med. Informat. Decis. Making*, vol. 21, no. 1, pp. 1–12, Dec. 2021, doi: 10.1186/s12911-021-01668-7.

[30] S. Fournier and E. Chappel, "Modeling of a piezoelectric MEMS micropump dedicated to insulin delivery and experimental validation using integrated pressure sensors: Application to partial occlusion management," *J. Sensors*, vol. 2017, pp. 1–7, Jan. 2017, doi: 10.1155/2017/3719853.

[31] M. H. Zarifi, H. Sadabadi, S. H. Hejazi, M. Daneshmand, and A. Sanati-Nezhad, "Noncontact and nonintrusive microwave-microfluidic flow sensor for energy and biomedical engineering," *Sci. Rep.*, vol. 8, no. 1, pp. 1–10, Jan. 2018, doi: 10.1038/s41598-017-18621-2.

[32] R. A. Peterfreund and J. H. Philip, "Critical parameters in drug delivery by intravenous infusion," *Expert Opinion Drug Del.*, vol. 10, no. 8, pp. 1095–1108, Aug. 2013, doi: 10.1517/17425247.2013.785519.

[33] D. C. Karnopp, D. L. Margolis, and R. C. Rosenberg, "Modeling, simulation, and control of mechatronic systems," in *System Dynamics*, 5th ed. 2012, pp. 77–161, doi: 10.1002/9781118152812.ch4.

[34] V. C. Rideout and D. E. Dick, "Difference-differential equations for fluid flow in distensible tubes," *IEEE Trans. Biomed. Eng.*, vol. 14, no. 3, pp. 171–177, Jul. 1967, doi: 10.1109/tbme.1967.4502495.

[35] J. Smyth, K. Smith, S. Nagrath, and K. Oldham, "Modeling, identification, and flow control for a microfluidic device using a peristaltic pump," in *Proc. Amer. Control Conf. (ACC)*, Jul. 2020, pp. 1360–1366, doi: 10.23919/ACC45564.2020.9147528.

[36] R. Zengerle and M. Richter, "Simulation of microfluid systems," *J. Micromech. Microeng.*, vol. 4, no. 4, pp. 192–204, Dec. 1994, doi: 10.1088/0960-1317/4/4/004.

[37] F. Moscato, F. M. Colacino, M. Arabia, and G. A. Danieli, "Pressure pulsation in roller pumps: A validated lumped parameter model," *Med. Eng. Phys.*, vol. 30, no. 9, pp. 1149–1158, Nov. 2008, doi: 10.1016/j.medengphy.2008.02.007.

[38] M. Li and J. G. Brasseur, "Non-steady peristaltic transport in finite-length tubes," *J. Fluid Mech.*, vol. 248, pp. 129–151, Mar. 1993, doi: 10.1017/S0022112093000710.

[39] Y. V. K. R. Kumar, S. V. H. N. K. Kumari, M. V. R. Murthy, and S. Sreenadh, "Unsteady peristaltic pumping in a finite length tube with permeable wall," *J. Fluids Eng.*, vol. 132, no. 10, Oct. 2010, doi: 10.1115/1.4002518.

[40] A. Small and P. Nagarani, "Fluid motion in finite length tubes in peristaltic pumps," in *Advances in Fluid Dynamics* (Lecture Notes in Mechanical Engineering). Singapore: Springer, 2020, doi: 10.1007/978-981-15-4308-1_3.

[41] Y. A. Elmaboud, K. S. Mekheimer, and S. I. Abdelsalam, "A study of nonlinear variable viscosity in finite-length tube with peristalsis," *Appl. Bionics Biomech.*, vol. 11, no. 4, pp. 197–206, 2014, doi: 10.3233/ABB-140101.

Lianqiao Zhou is currently pursuing the M.D. degree with the Institute of Mechanics, Chinese Academy of Sciences, Beijing, China.

His current research interests include mechanics of soft materials and structures, flexible sensors, and energy harvesters.

Qinlan Li is currently pursuing the Ph.D. degree with the Institute of Mechanics, Chinese Academy of Sciences, Beijing, China.

His current research interests include flexible sensors and energy harvesters.

Liyang Wang is an Embedded Systems Development Engineer at Tuoren Medical Device Research and Development Institute Company, Changyuan, China. His research interests focus on the design and development of medical device control systems.

Mengjie Wang is an Electronic Engineer at Tuoren Medical Device Research and Development Institute Company, Changyuan, China. Her research interests focus on the preparation and testing techniques of medical device control circuits.

Longfei Li is an Embedded Systems Development Engineer at Tuoren Medical Device Research and Development Institute Company, Changyuan, China. His research interests focus on the design and development of medical device control systems..

Bo Ding is a Mechanical Structural Design Engineer at Tuoren Medical Device Research and Development Institute Company, Changyuan, China. His research interests focus on the design of the drive structures for medical devices.

Shengwen Bao is an Embedded Systems Development Engineer at Tuoren Medical Device Research and Development Institute Company, Changyuan, China. His research interests focus on the design and development of medical device control systems.

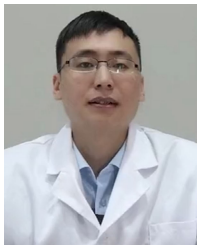

Shugang Wang is a Sensor Development Engineer at Tuoren Medical Device Research and Development Institute Company, Changyuan, China. His research interests focus on the design and manufacturing of medical sensors.

Xiaobing Xiao is a Senior Engineer at Tuoren Medical Device Research and Development Institute Company, Changyuan, China. His research interests focus on the design and preparation of medical devices.

Jingqiang Cui is a Senior Engineer at Tuoren Medical Device Research and Development Institute Company, Changyuan, China. His research interests focus on the design and development of antibacterial high-polymer materials and super-slippery materials.

Guosheng Wang is the Founder of Tuoren Medical Device Research and Development Institute Company, the President of the Henan Medical Device Association, a Professor at the Beijing University of Chemical Technology, and a master's research advisor. His research interests focus on the design and preparation of medical devices.

Chong Liu received the Ph.D. degree from the Hong Kong University of Science and Technology, Hong Kong, China, in 2011.

He is currently a Professor at the Institute of Mechanics, Chinese Academy of Sciences, Beijing. His research interests focus on micro-nano mechanics, high-temperature superconducting thin film preparation and characterization, and micro-nano scale fluid flow and heat transfer.

Yewang Su received the Ph.D. degree from Tsinghua University, Beijing, China, in 2011.

He is currently a Professor at the Institute of Mechanics, Chinese Academy of Sciences, Beijing. He is now finding the new application of flexible and stretchable sensors on wearable devices and the intelligent industry. He has been published more than 100 SCI articles in peer-reviewed high-level scientific journals and held more than 20 patents in his research area. His research focuses on flexible and stretchable sensors in the field of sensing the curvature, large strain, and pressure.